

HEAT TRANSFER IN SEPARATED FLOWS

by

Yiu-hung Liu

B. S., National Taiwan University, Taipei, Taiwan, 1963

A MASTER'S REPORT

submitted in partial fulfillment of the
requirements for the degree

MASTER OF SCIENCE

Department of Mechanical Engineering

KANSAS STATE UNIVERSITY

MANHATTAN, KANSAS

1968

Approved By:


Major Professor

LD
2023
R4
1968
L58
62

TABLE OF CONTENTS

List of Figures	1
Introduction	3
Heat Transfer in the Separated Flow over a Cavity	11
Heat Transfer in the Separated Flow over a Backward Facing Step	19
Heat Transfer in Rectangular Duct with Abrupt Enlargement	31
Heat Transfer in a Circular Duct with Separation	43
Discussions and Conclusions	52
Bibliography	58
Nomenclature	61
Acknowledgement	63

LIST OF FIGURES

Figure	Page
1. Cavity Separated Flow and Its Pressure Distribution.....	5
2. Flow Over a Backward Facing Step and Its Pressure Distribution.....	5
3. The Pressure Distributions for a Backward Facing Step.....	6
4. The Pressure Distribution for a Forward Facing Step.....	8
5. Flow Pattern in a Rectangular Duct.....	10
6. Pressure Coefficient on the Floor of Cavity.....	13
7. Variation of Ratio h/h_{fp} with x/L for Various Cavity Lengths.....	14
8. The Cavity Model of Seban.....	15
9. Heat Transfer Coefficient for the Surfaces of the Cavities.....	16
10. The Test Models of Seban et al.....	20
11. Heat Transfer Coefficient and Recovery Factor of Model A, Used by Seban et al.....	20
12. Heat Transfer Coefficient and Recovery Factor of Model B, Used by Seban et al.....	21
13. Heat Transfer Ratio Behind a Downstream Facing Step.....	21
14. a) Model Configuration and Dimensions Used by Chapman et al.....	23
b) Maximum Reynolds Number for Pure Laminar Type Separation.....	24
c) Maximum Reynolds Number for Pure Laminar Type Separation.....	25
15. Heat Transfer Coefficient Ratio of Two Models used by Naysmith.....	27

16.	Laminar Flow over a Backward Facing Step.....	29
17.	Local Heat Transfer Rate in the Separated Region.....	29
18.	The Configuration of the Model and Local Heat Transfer in the Separated Region.....	32
19.	Schematic Diagram of the Test Apparatus of Filetti and Kays.....	32
20.	Overall Stall Length as Measured by Abbott.....	34
21.	Nusselt Number Versus Normalized Distance for Short Stall and Long Stall.....	36
22.	Nusselt Number Versus Normalized Distance for Short Stall and Long Stall.....	37
23.	Nu/Nu_{∞} Versus Normalized Distance.....	38
24.	Nu/Nu_{∞} Versus Normalized Distance.....	38
25.	Flow Patterns, Heat Transfer Coefficients, and Temperature Recovery Factors for the Diffuser used by Baker et al.....	40
26.	Flow Patterns, Heat Transfer Coefficients, and Temperature Recovery Factors for the Diffuser used by Baker et al.....	41
27.	Variation of Point Unit Thermal Conductance in a Circular Tube with an Orifice.....	44
28.	Local Heat Transfer Coefficient in a Circular Pipe with Sudden Enlargement.....	46
29.	Local Heat Transfer Coefficient Downstream of a Rib in a Pipe with Uniform Heat Flux.....	46
30.	Local Heat Transfer Results in the Separated, Reattached, and Redevelopment Regions.....	48
31.	Local Heat Transfer Results in the Separated, Reattached, and Redevelopment Region.....	48
32.	Local Heat Transfer Results in the Separated, Reattached, and Redevelopment Region.....	50

- 33. Comparison of Heat Transfer Results for
Pr = 3 and Pr = 6.....50
- 34. Correlation of Peak Nusselt Number with
Orifice Reynolds number.....51

INTRODUCTION

Separated flows are flows which do not follow the guiding walls. Flow patterns in which the fluid breaks away from a guiding surface are encountered in the design of aerodynamic surfaces such as high speed aircrafts and missiles. Separated flows also occur where indentations or protuberances are present on the surfaces and where ribs or enlargements take place in ducts. Since the separated flow regions are of much more complex nature than ordinary boundary layer flow regions, the determination of local heat transfer coefficients and skin friction between the flow and the surface is not amenable to analytical solutions and most of the heat transfer results are obtained experimentally.

According to the geometry of the body, there are several main types of separated flows. The first type of separation occurs as a result of the flow over a cavity in a flat wall as shown in Fig. 1. This type of separated flow, cavity separation, is characterized by a separation point and a reattachment point. These two points depend on the geometry of the cavity. In this kind of separated flow the length of the cavity " L ", is limited by the depth " H " for if the length of the cavity is far greater than the depth, the reattachment point will be on the floor of the cavity and we encounter another type of separated flow. The pressure drops immediately after the separation point then remains constant over the separated region. As the flow approaches the reattachment

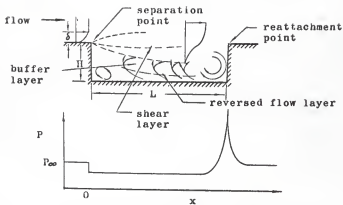


Fig. 1. Cavity separated flow and its pressure distribution.

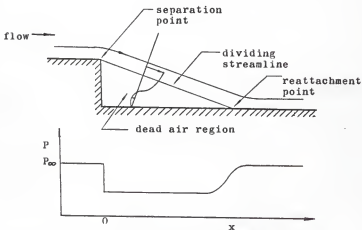


Fig. 2. Flow over a backward facing step and its pressure distribution.

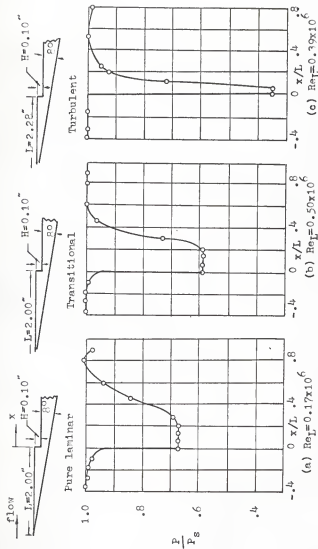


Fig. 3. The pressure distributions for a backward facing step; $N=2.3$ Reference (1).

point, the pressure rises and reaches a maximum value at that point. Part of the shear layer approaching the reattachment region will not have sufficient kinetic energy to negotiate the required pressure rise, and therefore, this part of flow is forced back to the separated region and forms the "dead air" region. In the "dead air" region, the velocity is very small compared with the free stream velocity and the pressure is uniform. There are vortices at the corners of the cavity.

The second type occurs during the flow over a surface with a forward facing or a backward facing step. Fig. 2 shows the flow over a backward facing step. In this case, the separation point is clearly defined geometrically. The pressure slightly decreases before the separation point and at this point it drops down suddenly to a minimum and then remains almost constant. As the flow approaches the reattachment region, the pressure increases up to a maximum value at the reattachment point. Fig. 3 shows the pressure distributions for laminar, transitional, and turbulent flows for a backward facing step.

Fig. 4 shows the separated flow over a forward facing step. In such a case the reattachment point is defined geometrically, whereas the separation point is not so clear. For laminar flow, the pressure begins to increase at some place before the separation point, and then increases gradually to a maximum at the reattachment point. If transition occurs in the separated region, the pressure also increases gradually after the initial pressure rise, but as the flow approaches

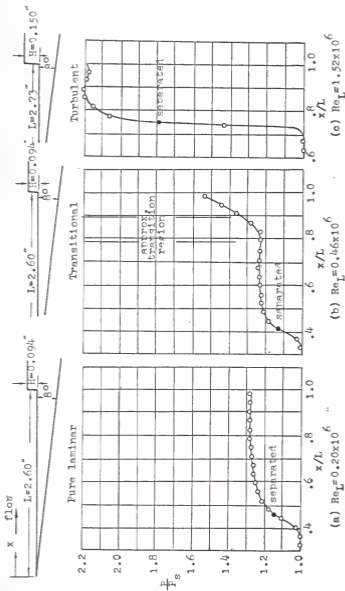


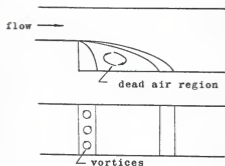
Fig. 4. The pressure distributions of forward facing step; $Re = 2.3$. Reference (1).

the reattachment region, the pressure increases rapidly to a maximum value at the reattachment point. For turbulent flow, the pressure rises very rapidly before separation point and reaches the maximum value at the reattachment point.

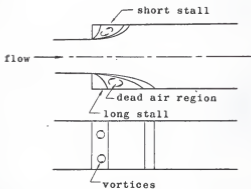
The third type of separation occurs in a duct as a result of different methods of construction as, for example, in pipe fittings, circumferential ribs and sudden enlargements of the duct crosssectional area. Abbott and Kline (2)¹ observed the flow in the separated region of subsonic turbulent flow for the system shown in Fig. 5. There are one or more vortices rotating about an axis normal to the horizontal floor in the small region next to the vertical wall. Adjacent vortices are counter-rotating and not necessarily of the same size and they may change in size with time. This is only a small part of the separated region. The main part is the "dead air" region where the fluid is circulating with a velocity comparatively smaller than the free stream. This circulatory flow appears to be steady and provides a velocity of the order of $1/5$ the free stream velocity. The pattern of pressure distribution is similar to that of a backward facing step separated flow.

This report will be concerned with reviewing and evaluating the state of the art of the heat transfer in separated flow regions for the different configurations discussed above.

¹Numbers in parantheses refer to references in bibliography.



(a)



(b)

Fig. 5. Flow pattern in a rectangular duct
with (a) single step
and (b) double step.
Reference (2)

HEAT TRANSFER IN THE SEPARATED FLOW OVER A CAVITY

Generally speaking the boundary layer equations are only valid as far as the point of separation. A short distance downstream from the separation point, the boundary layer becomes so thick that the assumptions which are made in the derivation of the boundary layer equations no longer apply. In 1956, Chapman (3) presented his well-known cavity separation theory. He assumed the cavity as an isothermal "dead air" sink to which heat was transferred through the shear layer, and disregarded the resistance between the inner wall and the fluid in the cavity. He obtained the average heat transfer coefficient over the whole separated region. Larson (4) reported his experimental results of heat transfer measurements in the cavity of Chapman's model. His results for laminar flow agreed well with the analysis of Chapman, but disagreed considerably for the turbulent flow. Three years later, Carlson (5) analysed the same problem by considering the effect of the floor surface and obtained the local heat transfer coefficients in the separated region. Carlson's results agreed with those obtained by Larson (4).

As mentioned earlier, for flow over a cavity, if the ratio of the cavity length "L" to the depth "H" (L/H) is greater than a certain value, the reattachment point will be on the floor of the cavity. It has been reported by Charwat (6), Seban (7) and others that for $L/H = 10$ to 12, the flow reattaches to the

floor of the cavity. Emery (8) experimentally found that reattachment took place at $L/H = 14$. The experiments of Emery (8) were conducted in a wind tunnel which had a measured center line Mach number of 2.86. The cavity was 0.25-in. deep by 0.75-in. wide with a length which varied from 0 to 5-in.. The cross section of the tunnel was 0.75-in. x 1.634-in.. Pressure profiles were made with a 2-mm pitot tube and static wall taps. The measured boundary layer thickness just prior to the expansion step was approximately 0.15-in. and the local Reynolds number $\sqrt[4]{}$ based upon a starting length " L_{st} " determined by $(\delta/L_{st} = 0.37 (Re)^{-1/5})^{1/4}$ was 11.4×10^6 . From his results, it was shown that there existed two distinct regions of flow, $L \leq 6H$ and $L \geq 6H$. The value of $x = 6H$ represented roughly the region of the cavity which was influenced by only the expansion step and $x > 6H$ was the region controlled primarily by the recompression step. A typical set of pressure coefficients along the cavity floor is shown in Fig. 6. It is seen that for $x < 5H$ the coefficient was essentially constant and only began to increase for x/H greater than 6. The values of the pressure coefficient P_c ,

$$P_c = (\frac{P}{P_\infty} - 1) / \frac{1}{2} M_\infty^2$$

where P_∞ and M_∞ were evaluated at the free stream prior to the expansion step, were presented as a ratio of P_c/P_{c1} , where P_{c1}

¹Reynolds number based upon the boundary layer thickness.

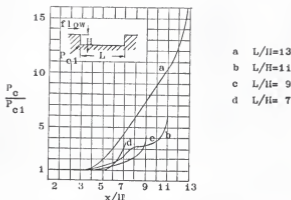


Fig. 6. Pressure coefficient on the floor of cavity. $M = 3$. Reference (8)

was determined from the above equation using the pressure measured at the base of the expansion step.

For the heat transfer coefficient measurements, the cavity surface was covered by a 0.016-in. stainless steel strip which was heated by electrical resistance heating. The transient temperatures produced by cooling were recorded on a single-pen strip chart recorder. Fig. 7 shows the results of the heat transfer coefficient of the rectangular cavity. For cavity lengths greater than $3H$ and less than $7H$, the heat transfer coefficient decreased slightly up to some point within $x/L=0.4$. For $x/L > 0.4$, h increased to its maximum value at $x/L = 1.0$. For these cavities, the heat transfer coefficient exceeded that of the flat plate within a region of approximately one step height ahead of the recompression step.

For $L/H > 7$, the trend of h noticeably changed. The

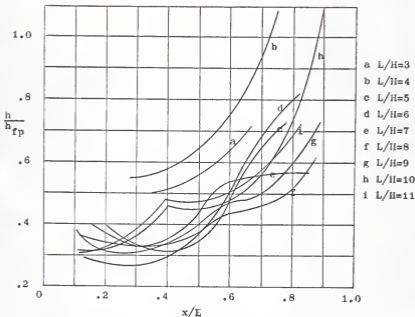


Fig. 7. Variation of ratio h/h_{fp} with x/L for various cavity lengths.. $M = 3$. Reference (8)

decrease to a minimum within $x/L = 0.4$ was still present, but the heat transfer coefficient tended to level out for one or two step heights, and then proceeded to increase. This apparently results from the cavity length becoming sufficiently large so that the region governed by the recompression step region is now essentially separated from the region influenced by the expansion step. As L/H increased, the maximum h increased from approximately 70 percent h_{fp} at $L/H = 7$ to 130 percent h_{fp} at $L/H \approx 10$ (h_{fp} was the flat-plate value at

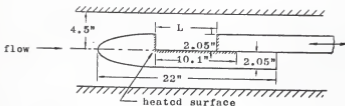


Fig. 8. The cavity model of Seban (7).
The length L was adjustable in 0.505-in.
increments up to $L = 10.10$ -in..

$x/H = -1$). As L/H became greater than 10, a distinct peak for h was found at $x/H = 4$. This was apparently the result of the onset of reattachment and indicated that the reattachment was becoming imminent.

The experimental test model used by Seban (7) for studying heat transfer in subsonic turbulent flow is shown in Fig. 8. It has a rectangular notch, 2.05-in. deep, with a variable length which could be varied from 4 to 10-in., by changing the downstream position of the back face. The tunnel was 6-in. wide. The air flow just upstream of the notch was at 160 fps with a boundary layer thickness of 0.005-in.. Results were obtained for velocities between 160 to 590 fps. The maximum difference between the wall and free stream stagnation temperatures was of the order of 20°F ; stagnation temperatures were of the order of 85°F . In Seban's experiments, L was 10-in. which was the maximum cavity length that can be attained without the point of reattachment shifting to the floor of the cavity.

Fig. 9 shows the data obtained Seban (7). The highest

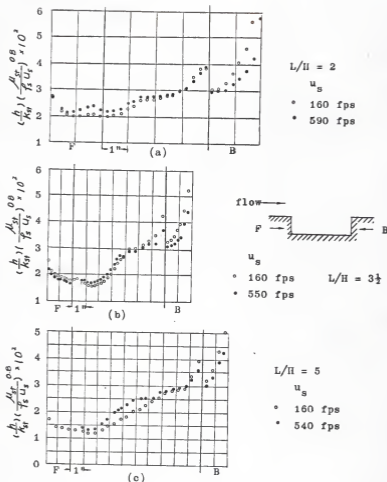


Fig. 9. Heat transfer coefficient for the surfaces of the cavities. The abscissa contains the front face (F), to the left; the back (B), to the right; and the bottom surface placed between these faces. Reference (7).

heat transfer coefficient occurred at the top of the back face, in the region of reattachment, and decreased with distance toward the bottom. As the flow turned the corner from the back face to the bottom, there was an increase in the local heat transfer coefficient. The results showed a drop in the heat transfer coefficient at the separation point and a minimum in the first half of the notch. The heat transfer coefficient increased near the recompression region with the increase of L/H , but decreased near the separation region.

The heat transfer coefficient was incorporated in the group $(h/k_{st})(\mu_{st}/\rho_s u_s)^{0.8}$. This selection was obviously guided by the form of correlation associated with turbulent flow over a flat plate, and the 0.8 power dependence on the velocity did exist but not all over the whole region. Though the average value of the coefficient for the entire separated region depended on the velocity raised to about the 0.6 power, the 0.8 power still was to some degree in the entire downstream region where the main heat transfer occurred. The value of the power may be changed for different reference points. Generally the reference values are taken at some point before separation. The heat transfer coefficient of the separated region is always referred to those of the attached boundary layer two to five notch depths ahead of the separation point, which are measured in the test, because the heat transfer is affected slightly by the expansion around the corner of the notch. Seban (7) suggested that if the density was taken at the stagnation

point instead of at the separation point a satisfactory degree of correlation could be achieved if the exponent of 0.8 was altered to 0.7.

HEAT TRANSFER IN THE SEPARATED FLOW OVER A BACKWARD FACING STEP

Seban, Emery, and Levy (9) studied the heat transfer in separated flow over a backward facing step with models having 0.81-in. and 0.25-in. step heights. Fig. 10 shows the test models used by Seban et al.. Each of the models was mounted centrally in and spanning the 6-in. width of the 6-in. by 9-in. closed test section of a wind tunnel. They were made of bakelite, being heated by means of electric current passing through nichrome ribbons which were 0.002-in. thick and 1-in. wide, affixed to the model surface with lengthwise dimension parallel to that of the flow. Air was used as the working fluid in all tests. Observations were made at various air speeds from 150 to 500 fps, with stagnation pressure near atmospheric pressure and stagnation temperatures of the order of 90°F. Without heating, adiabatic wall temperatures were observed. With heating, the temperature differences were of the order of 20°F, between wall surface and stagnation temperatures.

The local heat transfer coefficient was defined as:

$$h = q / (T_w - T_{aw})$$

In high speed flow, the direction of heat flow at the surface does not depend on the difference between the wall temperature and the free stream temperature as in low speed flow, but rather on the difference between the wall temperature and the adiabatic wall temperature. As a result in order to correlate the experimental data it is therefore convenient to define the

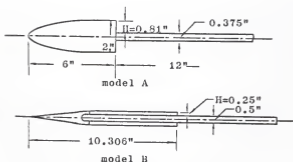


Fig. 10. The test models of Seban et al..
Reference (9).

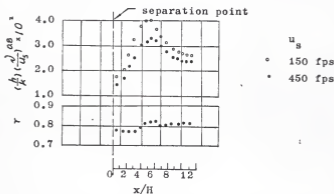


Fig. 11. Heat transfer coefficient, and recovery factor of model A used by Seban et al..
Reference (9).

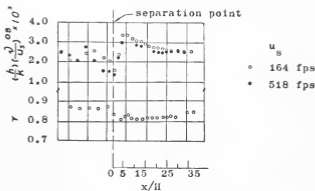


Fig. 12. Heat transfer coefficient and recovery factor of model B used by Seban et al.. Reference (9).

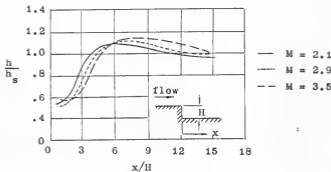


Fig. 13. Heat transfer ratio behind a downstream facing step obtained by Charwat. Reference (6).

heat transfer coefficient as shown before.

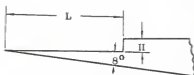
The recovery factor is defined as:

$$r = (T_{aw} - T_{\infty}) / (T_{st} - T_{\infty})$$

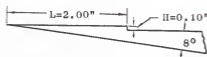
which is a measure of the fraction of the free stream dynamic temperature rise recovered at the wall.

The results obtained by Seban et al. (9) are shown in Figs. 11 and 12. The heat transfer coefficient decreased suddenly after the separation point and then increased to a maximum at the reattachment point. In the dead air region, the low velocity caused relatively low heat transfer rate. Generally the maximum value of heat transfer coefficient at the reattachment point is greater than that obtained just before separation. The position of this maximum value is quite difficult to fix. In Seban's tests, they occurred at about five step heights downstream from separation point for the model A and six step heights for model B.

The pattern of heat transfer data of a supersonic flow over a backward step are somewhat similar to those of subsonic as shown in Fig. 13. Charwat (6) reported these data without mentioning how he obtained the results and what kind of model was used. The minimum value of the heat transfer ratio occurred immediately behind separation and was followed by an increase, reaching a maximum at the reattachment point. In supersonic flow, one of the interesting problems is the stability of the flow. From many experimental observations, it was found that the stability of the separated laminar mixing layer increased



Model	L inches	H inches	L/H
A-1	1.14	0.041	27.8
A-2	2.60	0.094	27.7
A-3	2.73	0.150	18.2
A-4	3.30	0.150	22.0
A-5	6.55	0.237	27.7



B-1 model

Fig. 14a. Model configurations and dimensions.
Reference (1).

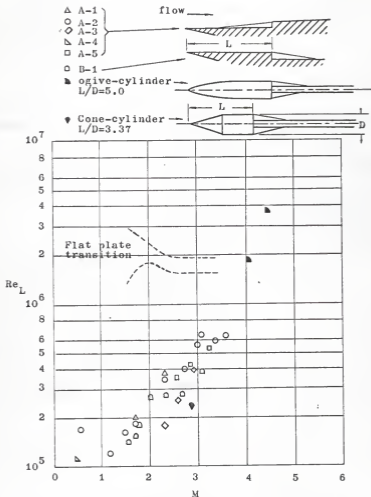


Fig. 14b. Maximum Reynolds number for pure laminar type separation. Reynolds number based on model length. Reference (1).

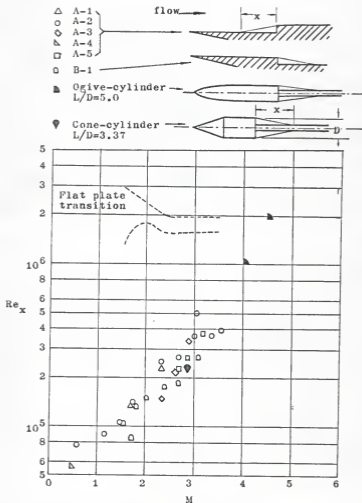


Fig. 14c. Maximum Reynolds number for pure laminar type separation. Reynolds number based on length of separated layer. Reference (1).

markedly with an increase in Mach number, so it became evident that the prevalence of pure laminar type separation increased as Mach number was increased. These results can be observed in Figs. 14a, 14b, and 14c which also show the configurations and dimensions of the models used in the experiments.

Naysmith (10) presented the results of two experiments designed to measure heat transfer at supersonic speeds in a region of separated flow behind backward facing steps. The first model tested was a 15° wedge terminating in a step about 1-in. high: this was mounted on the bottom wall of a 5-in. by 5-in. wind tunnel operating at $M = 4$. The boundary layer before separation was turbulent, and Mach number in the flow outside the boundary layer was about 2.9. The model was tested at 2 stagnation pressures, 3 atmospheres and 5 atmospheres, giving Reynolds numbers at the step of the order of 10^7 . The second model was designed to be used in the 3-ft. x 3-ft. wind tunnel. This model consisted of a 15° half-angle cone of 11-in. base diameter followed by a circular cylinder 9-in. in diameter. The step height of 1-in. was the same as that of the first wedge. This model was tested at a Mach number of 2.0, giving a local Mach number of 1.7 on the cone just before separation. Reynolds number (based on distance from cone apex) just before separation was only 2×10^6 and the boundary layer was laminar.

The heat transfer results of these two models are shown in Fig. 15. The heat transfer coefficient was defined as:

$$h = q / (T_{aw} - T_w)$$

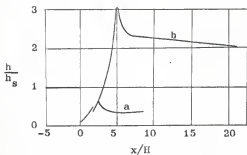
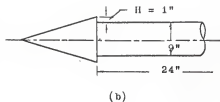
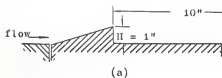


Fig. 15. Heat transfer coefficient ratio of two models used by Naysmith. Reference (10).

Fig. 15 shows that a peak exists in the value near reattachment and that h/h_g of the first model is less than unity after reattachment, but the number and spacing of the measuring stations were insufficient to determine the magnitude of the peak. There is a pronounced peak at reattachment of the second model. This was due to the fact that the boundary layer became turbulent after separation.

Rom and Seginer (11) used a shock tube to investigate the heat transfer to a two-dimensional backward facing step in laminar supersonic flow. The shock tube consisted of a cylindrical compression chamber 1.5 meter long and a square low pressure tube of 75 mm x 75 mm cross section, 7 meters long. The low pressure tube was evacuated to pressure of 0.35 mm Hg. abs.. High pressure bottled hydrogen or air were used as driver gases in the compression chamber. The model for heat transfer measurements was a steel plate having a sharp leading edge into which a step of height $H = 1.55$ mm was machined 14 mm behind the leading edge. The lower surface was machined to form the plate into a sharp wedge with an initial opening angle, at the leading edge of 9° . At the plate center ahead and behind the step, a groove was machined for insertion of the pyrex glass elements on which the thin platinum films (which were used to measure local heat transfer rate) were sputtered. The model is shown in Fig. 16. The shock Mach number ranged from 4 to 10 in these experiments. The corresponding flow Mach number were approximately 1.5 to 2.5 and Reynolds

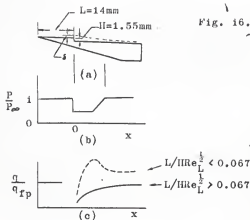


Fig. 16. Laminar flow over a backward facing step
 a) Physical flow field;
 b) schematic pressure distribution;
 c) schematic heat transfer distribution.
 Reference (11).

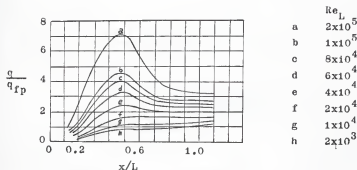


Fig. 17. Local heat transfer rate in the separated region.
 Reference (11).

numbers were varied between 2×10^3 to 2×10^5 . The heat transfer rates for Re_L from 2×10^3 to 2×10^4 were found to increase gradually through the reattachment zone as shown in Fig. 17. No peak of heat transfer was found in this range of Reynolds numbers except for the higher Reynolds numbers. The following relations were suggested for predicting the heat transfer rate:

- i. $q_x = 0.22 \left(H Re_L^{\frac{1}{2}} / L \right)^{1.3} \left(x/L \right)^{1.7}$
 when $\left(H Re_L^{\frac{1}{2}} / L \right) > 15$
 where q_x is the local value of the heat transfer rate from separation point to $x/L = 0.4$.
- ii. $q_{max} = 0.0465 \left(H Re_L^{\frac{1}{2}} / L \right)^{1.3} q_{fp}$
 when $\left(H Re_L^{\frac{1}{2}} / L \right) > 15$
 where q_{max} is the maximum heat transfer rate measured at the reattachment region.
- iii. $q_{ave} = 0.02 \left(H Re_L^{\frac{1}{2}} / L \right)^{1.3} q_{fp}$
 when $\left(H Re_L^{\frac{1}{2}} / L \right) > 15$
 $q_{ave} = 0.125 \left(H Re_L^{\frac{1}{2}} / L \right)^{0.8} q_{fp}$
 when $\left(H Re_L^{\frac{1}{2}} / L \right) < 15$
 where q_{ave} is the average heat transfer from the separation point to the end of the reattachment zone.

HEAT TRANSFER IN RECTANGULAR DUCTS WITH ABRUPT ENLARGEMENT

Seban (12) used the test model shown in Fig. 18 for studying the heat transfer in the separated flow region. The test surface was a bakelite plate, 12-in. wide and 18-in. long, which was one side of a rectangular channel $4\frac{1}{2}$ -in. by 12-in. in cross section. A step of one inch in height was placed at the upstream edge, so that the flow cross section there became $3\frac{1}{2}$ -in. by 12-in.. Heat was generated by electrical dissipation in ribbons placed lengthwise on the plate of test section. The temperature differences between the surface of the plate and the stream were of the order of 20°F . At 150 fps, the boundary layer just upstream of the step was turbulent. The local heat transfer coefficient was defined as:

$$h = q / (T_w - T_{\infty})$$

Fig. 18 shows the data obtained by Seban (12). The dashed line in this figure represents the heat transfer coefficient of the Seban's elliptical nose model as explained previously in Fig. 10. These two different models were tested under similar conditions. Both results are reproduced in Fig. 18 for the sake of comparison. The heat transfer coefficient of the elliptical nose model was greater than that of the rectangular duct over the separated region.

The heat transfer in the separated region behind a double backward facing step was reported by Filetti and Kays (13). Their test apparatus which is shown in Fig. 19, consisted of a

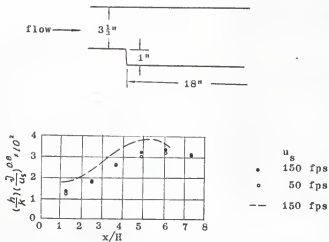


Fig. 18. The local heat transfer coefficient in the separated region of a rectangular duct and the configuration of the model used by Seban, Reference (12).

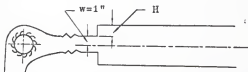
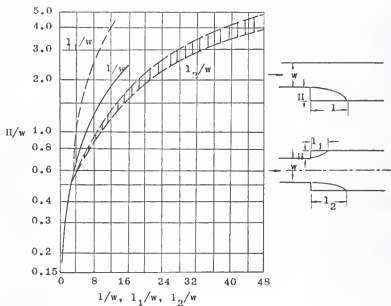


Fig. 19. Schematic diagram of the test apparatus of Filetti and Kays, Reference (13).

blower-plenum system delivering air to a plexiglass duct covering an instrumented flat plate. The apparatus was operated as an open loop, with the blower air inlet located some 10-ft. below the duct and plate, and the duct exhausting to the ambient in a large, lofty room. The maximum air delivery capacity of centrifugal blower was about 2000 cfm. Reynolds number was varied by throttling the blower at the inlet. The instrumented plate was slightly over 8-ft. long and was composed of 96 individual cells each about 1-in. long in the direction of airflow and 20-in. long transverse to the flow direction. Each cell was constructed from a rectangular cross sectional copper tube, insulated from the adjoining cells. The central 48 cells could be cooled by water and were each equipped with a Backman and Whitley heat flux transducer which measured heat flow from the surface to the coolant channel. All 96 cells were instrumented with iron-constantan thermocouples to measure surface temperature. Velocity profiles from which Reynolds numbers were determined were measured with a pitot-static probe at the outlet of the air-delivery duct. In operation, the test surface was close to water temperature and, thus, was essentially a constant temperature surface. Air temperature was about 20°F above water temperature.

One of the characteristics of this type of flow is that there are two stalls of different length on two duct walls respectively. This can be observed from both data of Abbott (2) and Filetti and Kays (13). Once the stall positions are



l/w = single step
 l_1/w = double step (short stall)
 l_2/w = double step (long stall)

Fig. 20. Overall stall length as measured by Abbott (2).

established, the long and the short stalls remained stable in their positions. Fig. 20 shows the experimental data of Abbott (2) for both the long and the short stalls of the double step configuration. From the results of Figs. 21 and 22, obtained by Filetti and Kays (13), one can see that the heat transfer rate distributions along the walls are not the same for the two different stalls and the value of Nu_{max} increased with an increase in the Reynolds number. The reattachment point is defined as the point where the maximum heat transfer occurred. The position of the maximum heat transfer obtained by Filetti and Kays was very close to the reattachment point obtained by Abbott (2) which is shown in dashed line in Figs. 21 and 22. The local heat transfer coefficient, the Nusselt number and the Reynolds number were defined by Filetti and Kays in their paper as:

$$h = q / (T_{st} - T_w)$$

$$Nu = hD_h/k$$

$$Re = uD_h/\nu$$

Figs. 23 and 24 show the ratio of the local Nusselt number of a separated flow and the Nusselt number for the heated wall of a fully developed flow in a flat duct at the same Reynolds number. The maximum heat transfer and the average heat transfer of the stalls were larger in the short stall than in the long one. Two empirical equations for predicting the maximum heat transfer were suggested by Filetti and Kays (13) as follows: for a short stall:

$$Nu_{max} = [0.124 + 0.101 \left(\frac{H}{W} \right)] Re^{0.689}$$

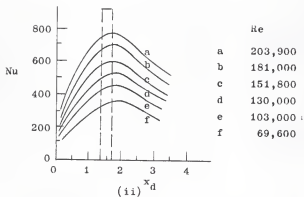
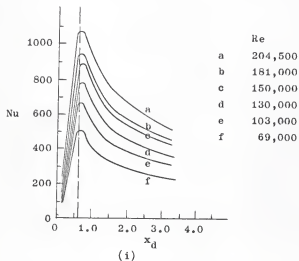


Fig. 21. Nusselt number versus normalized distance for (i) short stall; (ii) long stall. $H/w = 1.125$; $x_d = x/D_h$, where D_h defined as twice the plate spacing for the two horizontal parallel plates. Reference(13).

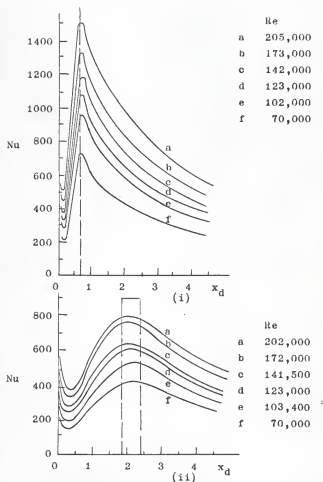


Fig. 22. Nusselt number versus normalized distance for (i) short stall; and (ii) long stall. $H/w = 2.1$, $x_d = x/D_h$, where D_h defined as twice the plate spacing for the two horizontal parallel plates. Reference (13).

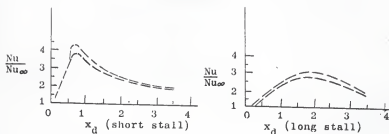


Fig. 23. Nu/Nu_{∞} versus normalized distance:
 $H/w = 1.125$; $x_d = x/D_h$.
 Reference (13).

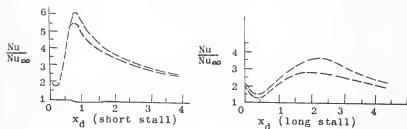
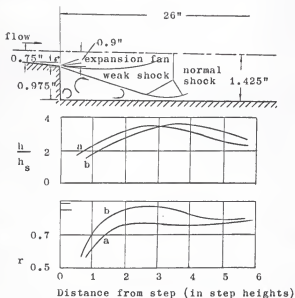


Fig. 24. Nu/Nu_{∞} versus normalized distance;
 $H/w = 2.1$; $x_d = x/D_h$.
 Reference (13)

for a long stall:

$$Nu_{\max} = \left[0.438 + 0.0695 \left(\frac{H}{W} \right) \right] Re^{0.593}$$

Baker and Martin (14) conducted experiments simialr to those of Filctti and Kays (13). Baker's model consisted of a convergent-divergent nozzle discharging into a parallel-sided diffuser. The nozzle had a throat cross-section 4-in. by 0.75-in. and an outlet cross-section 4-in. by 0.9-in.. The length of the divergent part was 0.976-in. and had a uniform taper of 5° . The nozzle area ratio of 1.2 resulted into a design outlet Mach number of 1.54 at an overall pressure ratio of 3.86. The actual Mach number at the main stream was determined from subsidiary experiments using a 16.5° wedge-shaped probe placed in the nozzle exit plane to create an attached oblique shock whose wave angle was measured. The diffuser is 26-in. long and its cross-section was 4-in. by 2.85-in.. It was connected to the nozzle so that their axis of symmetry coincided and the flow cross-section had a uniform width of 4-in. and also provided a backward facing step of height 0.975-in.. The upper horizontal surface of the diffuser was a mild steel plate with provisions for static pressure taps along its center line at $\frac{1}{2}$ -in. intervals. Heat transfer to the diffuser wall was measured by a number of copper-plastic units, of sandwich construction, set in the lower horizontal plastic surface along its center line, also at $\frac{1}{2}$ -in. intervals. Figs. 25 and 26 show the flow patterns and data obtained by Baker et al. (14). Baker reported the results for one side without any



Test conditions:

$M = 2.06$ at the edge of shear layer

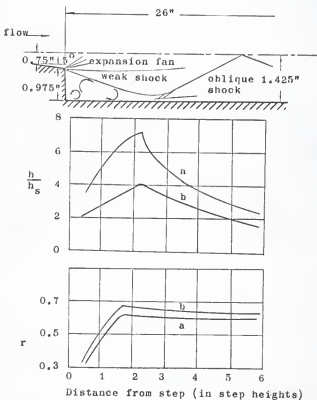
$M = 0.72$ at main stream

a. $Re = 9.63 \times 10^5$

b. $Re = 8.63 \times 10^5$

laminar flow

Fig. 25. Flow patterns, heat transfer coefficient and temperature recovery factors for the diffuser used by Baker et al.. Reference (14).



Test conditions:

$M = 2.23$ at the edge of shear layer

$M = 1.26$ at main stream

a. $Re = 1.08 \times 10^6$

b. $Re = 1.01 \times 10^6$

laminar flow

Fig. 26. Flow patterns, heat transfer coefficients and temperature recovery factors for the diffuser used by Baker et al.. Reference (14).

information about whether it was the long stall or the short one. One important object of Baker's paper was to observe the effect of transition on heat transfer. The maximum heat transfer ratio increased from about 3.5 to 3.9 as Reynolds number changed from 8.63×10^6 to 1.01×10^6 , but as Reynolds number increased from 1.01×10^6 to 1.08×10^6 , the maximum value of the ratio increased from 3.9 to 7.19. The sudden increase of heat transfer was due to transition which occurred somewhere near $Re = 1.08 \times 10^6$. When Reynolds number is such that the transition from laminar flow to turbulent flow occurs along the separated shear layer, the peak heat transfer in the reattachment region is much higher than that when the separated flow is wholly laminar or wholly turbulent.

HEAT TRANSFER IN A CIRCULAR DUCT WITH SEPARATION

Separation occurs in a circular duct and may be found in a wide variety of practical situations, e.g. at abrupt expansions and contractions of cross-sectional areas, in rapidly diverging sections, upstream and downstream of orifices, and at baffles etc.. In 1948, Boelter (15) presented the distribution of heat transfer rate in the entrance section of a circular tube. Among those different kinds of models, two orifices were used and separation occurred behind the orifice as the flow passed through it. The apparatus used by Boelter was essentially a doubly steam-jacketed tube through which air flowed and was heated. The saturated steam in the inner jacket surrounding the test pipe was condensed by losing heat to the air and was collected at 19 sections along the tube. Heat loss from this inner jacket to the surrounding atmosphere was prevented by the outer jacket containing steam at the same temperature. The rate of condensation of the steam obtained in each section was a measure of the heat transfer rate occurring in that section. By also measuring the tube wall temperature, the inlet temperature of the air, and the weight rate of air flow, the unit thermal conductance for several entrance condition and its variation with length was obtained. The test pipe was a highly polished seamless steel tube 32-in. long having a 2-in. outside diameter (1.785-in. I.D.). Partitions were brazed to the tube at approximately 1-in. intervals from

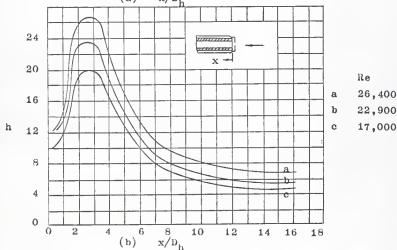
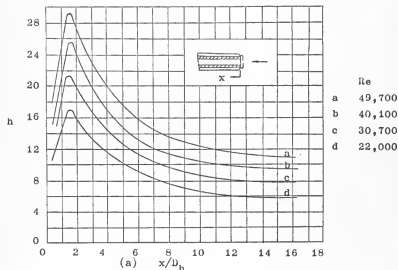


Fig. 27. Variation of point unit thermal conductance in circular tube with (a) $d_o/D = 0.84$
(b) $d_o/D = 0.56$, by Boelter. Reference (15).

the leading edge for a distance of 8-in. and then at 2-in. intervals for the remaining length of the tube, to yield 19 separately heated sections. These heated sections contained steam which was condensing because of the heat transfer through the wall of the tube to the cool air. Fig. 27 shows the data of Boelter (15). The heat transfer rate increased with an increase in Reynolds number, and a maximum heat transfer rate did exist.

Emerson (16) investigated the heat transfer in a circular tube with ribs and abrupt enlargements. All the experiments were performed with pipes of circular section and with air as the heat transfer medium. The velocity profile of the air arriving at the site of the geometrical feature whose effect was being examined was always fully developed. The internal diameter of the pipe in which all the local measurements were made was 3-in.. The pipe used for experiments was constructed from an epoxy resin loaded with powdered glass and reinforced with a woven glass tape. Heating was provided by means of ribbons of a 36 percent nickel-iron alloy 0.1-in. wide and 0.002-in. thick located circumferentially on the inner surface of the pipe. The temperature difference between the pipe surface and the fluid was about 15°C to 20°C. Emerson's results are shown in Figs. 28 and 29. The local heat transfer coefficient was defined as:

$$h = q / (T_w - T_b)$$

where T_b is the bulk temperature. The heat transfer

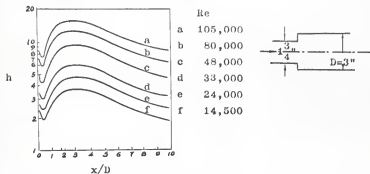


Fig. 28. Local heat transfer coefficients with air in a 3-in. diameter pipe downstream from a step change from $1\frac{3}{4}$ -in. diameter. Reference (16).

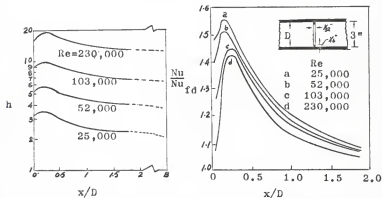


Fig. 29. Local heat transfer coefficient downstream of a rib in a pipe with uniform heat flux. Reference (16).

coefficients increased as the Reynolds numbers increased. The results from the experiments with a rib in a pipe with uniform heating are shown in Fig. 29, and there is a distinct peak in the heat transfer coefficient some eight to twelve rib heights downstream.

Krall and Sparrow (17) studied the heat transfer in separated flow due to an orifice. Their experiments were performed using a pressurized closed loop system. The essential components of the loop were a pump, an unheated starting length, the test section, a heat exchanger, a flowmeter, and a power supply. The unheated starting length and the test section were both fabricated from type 304 stainless-steel tubing having an internal diameter of 0.752-in. and a wall thickness of 1/16-in.. The test section was electrically and thermally isolated from its upstream and downstream neighbors by insulating bushings. Heating of the test section was accomplished by passing a-c electric current axially through the wall of the stainless-steel tube. Temperatures on the outer surface of the test section were measured by thermocouples which were affixed to the tube wall with copper oxide cement. These thermocouples were situated at 32 axial stations along the length of the tube. The spacing between adjacent couples was smallest near the upstream end of the tube where the effects of flow separation were expected to be largest. The Reynolds number range during the investigation varied from 10,000 to 13,000.

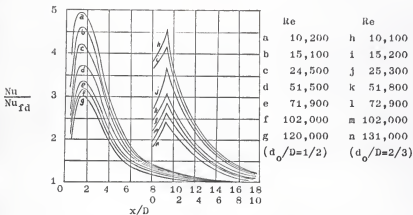


Fig. 30. Local heat transfer results in the separated, reattached, and redevelopment regions; $Pr=3$. Reference (17).

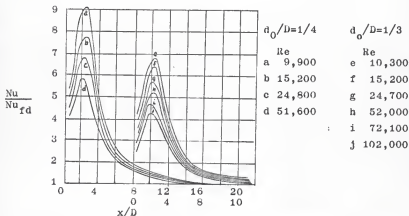


Fig. 31. Local heat transfer results in the separated, reattached, and redevelopment regions; $Pr=3$. Reference (17)

The local heat transfer coefficient h was defined as:

$$h = q / (T_w - T_b)$$

where T_b is the bulk temperature. Nusselt number and Reynolds number were based on the diameter of the test section. The results of Krall and Sparrow, Figs. 30 and 31, show the heat transfer in the test section for different Reynolds numbers and d_o/D ratios for constant Prandtl number. One can see that Nu/Nu_{fd} increased with the decrease of Reynolds number. At higher Reynolds numbers, there were relatively little effect on the ratio Nu/Nu_{fd} with further increases in Reynolds number. Thus for instance, for the $d_o/D = \frac{1}{2}$ orifice, the range of the peak values of Nu/Nu_{fd} was from 3.7 to 5 over Reynolds number range of 51,500 to 10,200. However, the peak values only changed from 3 to 3.3 when Reynolds number varied from 120,000 to 71,900. For fixed Reynolds number and Prandtl number, the maximum heat transfer varied with the d_o/D ratio. The curves of $d_o/D = 2/3$ in Fig. 30, for the weakest separation, were quite sharp at the reattachment point, while those for the stronger separations were rounded. This is due to the fact that for the smaller d_o/D ratio, the reattachment is somewhat spread out as a result of more violent eddies. Generally, the length of the separated region becomes longer with a decrease in the d_o/D ratio.

Fig. 32 shows the heat transfer results for $Pr = 6$. The comparisons of the heat transfer at different Prandtl numbers are shown in Fig. 33. The values of heat transfer for the lower

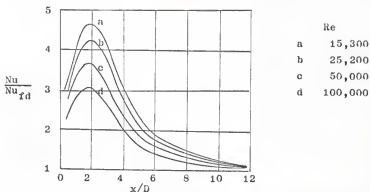


Fig. 32. Local heat transfer results in the separated, reattached, and redevelopment regions;

$Pr = 6$, $d_o/D = 1/2$.

Reference (17).

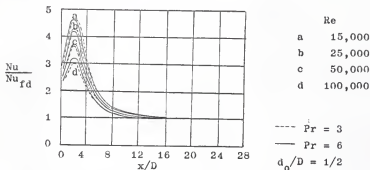


Fig. 33. Comparison of heat transfer results for $Pr = 3$ and $Pr = 6$.

Reference (17)

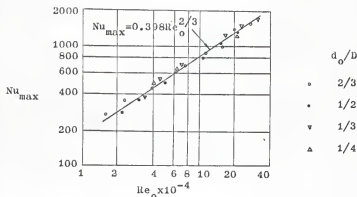


Fig. 34. Correlation of peak Nusselt number with orifice Reynolds number. Reference (17).

Prandtl numbers were greater than those for higher Pr , but as Reynolds number decreased to some value (e.g. $Re = 25,000$) the inverse effect was observed after the reattachment point. Also for all values of Reynolds number, the heat transfer coefficients obtained for $Pr = 3$ and 6 , were identical far downstream from the separation point (about six or eight diameter downstream from separation).

The peak Nusselt numbers for various separated conditions and the tube Reynolds numbers were brought together in Fig. 34. The abscissa is Reynolds number Re_o based on the orifice bore diameter d_o . It may be observed that the data are well correlated by this type of representation. The solid line in the figure has been selected as the best fit of the experimental results. It was found that Nu_{max} can be represented by:

$$Nu_{max} = 0.398 Re_o^{2/3}.$$

DISCUSSIONS AND CONCLUSIONS

From the literature survey conducted in this report, one common behaviour in the heat transfer characteristics in separated flow regions, in the various geometrical configurations considered, was observed. Results indicated that a drop in the heat transfer coefficient h occurs after the separation. Also there was an increase in the heat transfer coefficient near the reattachment region. After the peak value is reached, the heat transfer coefficient starts to decrease. It is not surprising to find a peak in the heat transfer rate near the reattachment, because the reattachment of the streamlining dividing the separated region from the flow outside is accompanied by a pressure rise in the boundary layer and a compression in the external stream, giving what may be compared with a stagnation point in this region, and hence a local peak in the heating rate. Since the heat transfer coefficient attains its maximum value in a very narrow range, it is possible that some experiments have failed to measure it if the model had a good heat-conducting surface. The information on heat transfer to and across the separated region is difficult to compare because of differences in test conditions and in the geometry of the models.

The heat transfer in the separated region is a function of Reynolds number, Prandtl number, and the geometry of the model. Generally, Prandtl number can be treated as constant for a specific model if the working fluid is the same in the

experiments. Hence Reynolds number and the geometry of the model become the main important factors that control the transfer of heat.

For the cavity flow, Emery (8) conducted all his experiments at a fixed Mach number and changed the length of the cavity to observe the dependence of the heat transfer coefficient over the cavity on the ratio of the cavity length to the height, L/H . When $L/H < 7$, the heat transfer coefficient decreases to a minimum at about $x/L = 0.4$ and then increases to a maximum value at $x/L = 1$. As the value of L/H increases, there is still a minimum at $x/L = 0.4$ but the heat transfer coefficient tends to level out for some distance before it increases to the maximum value. The maximum value of heat transfer coefficient increases with the increase of L/H . It was also found that the value of $x = 6H$ represented roughly the region of the cavity which was influenced by only the expansion step and $x > 6H$ was the region controlled primarily by the recompression step. No correlation was suggested by Emery (8). Seban (7) measured the heat transfer coefficient of all the three surfaces of the rectangular cavity. A maximum heat transfer coefficient h was observed at the top of the back surface (reattachment point). Another peak value of h was found at $x/L \rightarrow 1$ on the bottom surface. This is due to the fact that the flow forced into the cavity by the high pressure, comes down along the back surface of the cavity and reattaches with the bottom surface. Sometimes, there are vortices near the corner.

This can also increase the heat transfer rate. When the ratio L/δ increased, the heat transfer coefficient was found to increase near the recompression region while it decreases near the separation region.

For the backward facing step, the experimental results of Seban et al. (9) show that the position of the maximum heat transfer coefficient depends only on the step height. It remains almost at the same spot for the same step height even though Reynolds number is changed. The value of the heat transfer coefficient increases with an increase in the value of Reynolds number and also with an increase in the step height. The 0.8 power dependence of the heat transfer coefficient on the velocity is maintained to some degree in the entire separated region. The maximum heat transfer coefficient appearing at the reattachment point is a characteristic feature of all the results of Seban. A maximum in the heat transfer coefficient was also observed in Naysmith's results for supersonic flow. A maximum in the heat transfer coefficient occurred in all types of flow patterns in a separated flow in this paper (e.g. laminar, transitional, and turbulent flows). The largest value of the maxima for all flow patterns occurred for a laminar flow that changed into a turbulent flow over the separated region. Rom and Seginer (11) showed that there was no peak in the heat transfer coefficient for low Reynolds number (e.g. $Re < 2 \times 10^4$ in their experiment). A parameter $L/\delta Re_L^{\frac{1}{2}}$ was given, and when $L/\delta Re_L^{\frac{1}{2}}$ was greater than 0.067, no peak was

found at reattachment. Empirical relations suggested by Rom and Seginer in laminar supersonic flow over a backward facing step for predicting the heat transfer rate are:

$$\begin{aligned}
 & \text{i. } q_x = 0.22 \left(H \operatorname{Re}_L^{\frac{1}{2}} / L \right)^{1.3} \left(x/L \right)^{1.7} \\
 & \text{ii. } q_{\max} = 0.0465 \left(H \operatorname{Re}_L^{\frac{1}{2}} / L \right)^{1.3} q_{fp} \\
 & \text{iii. } q_{ave} = 0.02 \left(H \operatorname{Re}_L^{\frac{1}{2}} / L \right)^{1.3} q_{fp} \quad \left. \begin{array}{l} \text{---} \\ \text{---} \end{array} \right\} \text{when } (H \operatorname{Re}_L^{\frac{1}{2}} / L) \geq 15 \\
 & \quad q_{ave} = 0.125 \left(H \operatorname{Re}_L^{\frac{1}{2}} / L \right)^{0.8} q_{fp} \quad \text{when } (H \operatorname{Re}_L^{\frac{1}{2}} / L) < 15
 \end{aligned}$$

In a single backward step flow, the characteristics of heat transfer are similar to those of a backward facing step, but with a lower heat transfer coefficient. In a double backward facing step, there were two stalls of different length and the heat transfer rates were not the same between them.

Table 1 summarizes some of the results of Filetti and Kays (13).

Table 1

stall	step height	x_d at Nu_{\max}	Re	Nu_{\max}
short stall	1.125"	0.6	204,500	1080
	2.1"	0.7	205,000	1500
long stall	1.125"	1.4-1.7	203,900	780
	2.1"	1.8-2.4	202,000	800

One can see that the maximum value in the heat transfer coefficient is related to the step height. Nu_{\max} and the lengths of the stalls increase with an increase in the step height in both of the long stall and the short stalls. The relations for predicting the Nu_{\max} suggested by Filetti and Kays (13) are:

for a short stall:

$$Nu_{\max} = \left[0.124 + 0.101 \left(\frac{H}{W} \right) \right] Re^{0.689}$$

for a long stall:

$$Nu_{\max} = \left[0.438 + 0.0695 \left(\frac{H}{W} \right) \right] Re^{0.593}$$

From the results of Baker and Martin (14), the effect of transition from laminar to turbulent can be observed to be similar to the results of Naysmith (10).

The heat transfer over the separated region inside a circular duct due to an orifice, a rib, or sudden enlargement, is quite similar to that which occurs in the backward facing step. The results of Krall and Sparrow (17) for a circular duct with an orifice are shown in the following table from which one can observe an increase in $(Nu/Nu_{fd})_{\max}$ with a decrease of d_o/D .

Table 2

d_o/D	$(Nu/Nu_{fd})_{\max}$	conditions
2/3	4.2	Re = 15,200 Pr = 3
1/2	4.6	
1/3	6.6	
1/4	7.7	

They also suggested the following empirical equation for Nu_{\max} .

$$Nu_{\max} = 0.398 Re_o^{2/3}$$

Nu_{\max} was independent of the ratio of d_o/D . Besides the effect of geometrical configuration, the correlations of Filetti and Kays (13) and Krall and Sparrow (17) were almost the same. Since Krall's experiments were carried out in a circular tube,

and the Nusselt numbers presumably represented the average values around the tube periphery, thus he did not distinguish the separated contributions from the long and short stalls.

BIBLIOGRAPHY

1. Dean R. Chapman, Donald M. Kuchn, and Howard K. Larson.
"Investigation of Separated Flows in Supersonic
and Subsonic Streams with Emphasis on the Effect of
Transition." NACA TN 3869 March, 1957.
2. D. E. Abbott, and S. J. Kline. "Experimental Investigation
of Subsonic Turbulent Flow over Single and Double
Backward Facing Step." Journal of Basic Engineering,
ASME Transactions. Vol.64:3 September, 1962.
pp.317-325.
3. Dean R. Chapman. "A Theoretical Analysis of Heat Transfer
in Regions of Separated Flow." NACA TN 3792, 1965.
4. Howard K. Larson. "Heat Transfer in Separated Flows."
Journal of the Aero/Space Sciences. Vol. 26, No.11,
November, 1959. pp.731-738.
5. W. O. Carlson. "Heat Transfer in Laminar Separated and Wake
Flow Regions." Heat Transfer and Fluid Mechanics.
Institute. Stanford University Press, pp. 140-155,
1959.
6. A. F. Charwat, J. A. Dewwy. "An Investigation of Separated
Flows. Part II. Flow in the Cavity and Heat
Transfer." Journal of the Aero/Space Sciences. Vol.28,
No.7, 1961. pp.513-527.
7. R. A. Seban. "Heat Transfer and Flow in a Shallow
Rectangular Cavity with Subsonic Turbulent Air Flow."
International Journal Heat and Mass Transfer. Vol.8,

November, 1965. pp.1353-1368.

6. A. F. Emery, J. A. Sadunas, and M. Loll. "Heat Transfer and Pressure Distribution in Open Cavity Flow." Journal of Heat Transfer Transaction of the ASME. February, 1967. pp.103-108.
9. R. A. Seban, A. Emery, and A. Levy. "Heat Transfer to Separated and Reattached Subsonic Turbulent Flows Obtained Downstream of a Surface Step." Journal of the Aero/Space Sciences. Vol.26, No.12, December, 1959. pp.809-814.
10. A. Naysmith. "Measurements of Heat Transfer in Bubbles of Separated Flow in Supersonic Air Stream." ASME International Heat Transfer Conference. Part II, 1961. pp.378-381.
11. Josef Rom, and Arnan Seginer. "Laminar Heat Transfer to a Two-Dimensional Backward Facing Step from the High-Enthalpy Supersonic Flow in the Shock Tube." AIAA Journal Vol.2, No.2, February, 1964. pp.251-255.
12. R. A. Seban. "Heat Transfer to the Turbulent Separated Flow of Air Downstream of a Step in the Surface of a Plate." Journal of Heat Transfer, ASME Transactions. May, 1964. pp.259-264.
13. E. G. Filcetti, and W. M. Kays. "Heat Transfer in Separated Reattached, and Redevelopment Regions Behind a Double Step at Entrance to a Flat Duct." Journal of Heat Transfer, ASME Transactions. 9, 1967. Paper No.

66-Wa/HT-18.

14. P. J. Baker, and B. W. Martin. "Heat Transfer in Supersonic Separated Flow over a Two Dimensional Backward Facing Step." International Journal Heat and Mass Transfer. Vol.9, No.10, 1966. pp.1081-1088.
15. L. M. K. Boelter, G. Young, and H. W. Iverson. "An Investigation of Aircraft Heater, XXVII - Distribution of Heat Transfer Rate in the Entrance Section of a Circular Tube." NACA TN 1451, 1948.
16. W. H. Emerson. "Heat Transfer in a Duct in Region of Separated Flow." 3rd International Heat Transfer Conference held in Chicago Vol.1, 1966. pp. 267-275.
17. K. M. Krall, and E. M. Sparrow. "Turbulent Heat Transfer in the Separated, Reattached, and Redevelopment Regions of a Circular Tube." Journal of Heat Transfer, ASME Transactions. February, 1966. pp.131-136.

NOMENCLATURE

C_p	Specific heat at constant pressure
d_o	orifice bore diameter
D	diameter
D_h	hydraulic diameter
h	heat transfer coefficient
H	step height, or depth of cavity
k	thermal conductivity
l	total length of separation
L	flat plate length ahead of step, or length of cavity
P	pressure
P_c	pressure coefficient
q	heat flow rate per unit area
T	temperature
u	velocity
x	horizontal distance measured from separation point
w	one half the duct height

Dimensionless group

M	Mach number
Nu	Nusselt number, hL/k
Pr	Prandtl number, $C_p \mu / k$
r	temperature recovery factor
Re	Reynolds number, uD/μ , or uL/ν

Greek Symbol

γ	ratio of specific heats C_p/C_v
ρ	fluid density
μ	dynamic viscosity
ν	kinematic viscosity
δ	boundary layer thickness

Subscripts

aw	adiabatic wall conditions
fd	fully developed conditions
fp	flat plate conditions
o	orifice
s	condition ahead of separation point
st	stagnation point conditions
w	wall conditions
∞	free stream conditions

ACKNOWLEDGEMENT

The author would like to express sincere gratitude and indebtedness to Dr. Azer, his major professor, for his untiring valuable suggestions, corrections and criticism toward the completion of this paper, in spite of a very busy schedule.

HEAT TRANSFER IN SEPARATED FLOWS

by

Yiu-hung Liu

B. S., National Taiwan University, Taipei, Taiwan, 1963

AN ABSTRACT OF A MASTER'S REPORT

submitted in partial fulfillment of the
requirements for the degree

MASTER OF SCIENCE

Department of Mechanical Engineering

KANSAS STATE UNIVERSITY

MANHATTAN, KANSAS

1968

ABSTRACT

Published literature on heat transfer in separated flows was surveyed for different geometrical configurations under various flow conditions. The flow over a cavity, a backward facing step and through ducts with sudden enlargements were considered. It was observed that there was a common behaviour in heat transfer characteristics among these types of separated flows. Results indicated that a drop in the heat transfer coefficient h occurs after the separation point as compared to its value ahead of separation. Also, there was an increase in the heat transfer coefficient near the reattachment region. In general, the heat transfer coefficient in the separated flow region is a function of Reynolds number, Prandtl number and geometry of the model. The correlations, suggested by various authors, for predicting the heat transfer coefficients in the separated flow regions, were discussed.